# RAPID MAPPING OF SLOPE HAZARDS WITH PHOTOS ACQUIRED FROM A LOW-COST UNMANNED AERIAL VEHICLE USING THE AUTOMATIC MISSION PLANNING AND IMAGE PROCESSING SYSTEM (AMPIPS) - EXAMPLES OF NAMASHA AND LAONUNG AREAS

Cheng-Chien Liu[*1], Po-Li Chen[2], Chen-Yu Chen[3], Mei-Chei Chen[4] and Hsiao-Yuan Yin[5]

[1]Professor, Department of Earth Sciences,
Director, Global Earth Observation and Data Analysis Center,
National Cheng Kung University, No. 1, University Road, Tainan 701 Taiwan; Tel: +886-6-2757575#65422;
E-mail: ccliu88@mail.ncku.edu.tw

[2]Division Head, Global Earth Observation and Data Analysis Center,
National Cheng Kung University, No. 1, University Road, Tainan 701 Taiwan; Tel: +886-6-2366740;
E-mail: cygnuschen@gmail.com

[3]Soil and Water Conservation Bureau, Council of Agriculture, No.6, Guanghua Rd., Nantou City, Nantou County 54044, Taiwan; Tel: +886-49-2347410;
E-mail: cychen@mail.swcb.gov.tw

[4]Soil and Water Conservation Bureau, Council of Agriculture, No.6, Guanghua Rd., Nantou City, Nantou County 54044, Taiwan; Tel: +886-49-2347410;
E-mail: meichei99@mail.swcb.gov.tw

[5]Soil and Water Conservation Bureau, Council of Agriculture, No.6, Guanghua Rd., Nantou City, Nantou County 54044, Taiwan; Tel: +886-49-2347410;
E-mail: sammya@mail.swcb.gov.tw

**KEY WORDS:** UAV, Slope Hazard, Orthorectification, Mapping, Mission Planning, Image Processing

**ABSTRACT:** Slope hazards are destructive geological processes that cause enormous damage to human settlements, roads, infrastructure, and other valuable resources. Triggered by earthquake or heavy rainfall, the slope hazards are usually occurred in hilly regions over large areas yet within short period of time. Rapid mapping of the slope hazards is therefore a crucial task for disaster mitigation, assessment and relief. Among the general air-borne and space-borne platforms, the unmanned aerial vehicle (UAV) provides an innovative approach that is much cheaper, safer and more flexible to be deployed in a small area, ranged from a few to tens of square kilometers. Even on a overcast day, flying an UAV at low altitude is still able to give us a good dataset for mapping the disaster area. However, there is a significant gap in recording the accurate position and attitude data during an UAV flight mission. As a result, a lot of UAV platforms are limited to qualitative applications using non-georeferenced photos. Thanks to our recent progress in developing the automatic mission planning and image processing system (AMPIPS), we successfully employ a low-cost UAV in Namasha and Laonung areas to acquire tens of photos from approximately 800 meters. Comparing to the control points extracted from the base image, the accurate position and attitude of camera can be accurately derived when each photo is shot. Together with the digital topography model, the standard procedure of orthorectification can be applied to process each photo. All orthorectified photos are then stitched to a seamless and color-balanced mosaic and published onto Google Earth. This research demonstrates that the orthorectified image of slope hazards can be rapidly generated using a low-cost UAV with AMPIPS, and the result can be shared and browsed in 3D fashion through the internet.

## 1. INTRODUCTION

Unmanned Aerial Vehicle (UAV) provides an innovative approach of remote sensing that is much cheaper, safer and more flexible to be deployed in a small area, ranged from a few to tens of square kilometers. Civilian applications of UAV is therefore progressing fast, such as wildfire monitoring, earth science, humanitarian rescue, agriculture, environment, disaster assessment, survey, etc. Since all photos/data acquired by these low-cost UAVs need to be georeferenced for further applications, to develop a fast and reliable approach to georeferencing these photos/data plays one of the key roles of blooming the civilian market of low-cost UAV (Zhou, Li, and Cheng 2005). For the case of low-cost UAV platform, however, there is a significant gap in recording the accurate position and attitude data during its flight mission. The existing position/attitude sensors available are not only too heavy but also too expensive

to be loaded on a low-cost UAV. As a result, a lot of low-cost UAV platforms are limited to qualitative applications using non-georeferenced photos (Jones IV, Pearlstine, and Percival 2006).

Various approaches were integrated and implemented in the UAV automatic mission planning and image processing system (AMPIPS), which allows the users to plan a flight mission and generate three levels of geo-referenced products (Liu 2011). To support the rapid mapping of slope hazards in Taiwan area, Global Earth Observation and Data Analysis Center (GEODAC) at National Cheng-Kung University employed AMPIPS to process the photos acquired from CropCam® (see Fig. 1). CropCam® is a fixed-wing glider equipped with an autopilot system that is commercially available at comparatively lower cost. Table 1 gives the detailed specification of CropCam®. This paper gives two examples of rapid mapping of slope hazards at Namasha (17 June 2011) and Laonung (9 June 2011) areas, as well as the assessment of their planimetric accuracy.

TABLE 1 SPECIFICATION OF CROPCAM

| | |
|---|---|
| Wing span | 2.44 m |
| Length | 1.22 m |
| Weight | 2.72 kg |
| Payload | 400 g |
| Engine | Brushless electric motor |
| Cruise speed | 50 - 80 km/hr |
| Batteries | Lithium Polymer |
| Flight duration | 25 min |

Figure 1. CropCam®.

## 2. MISSION PLAN AND IMAGE PROCESSING

### 2.1 Flight plan

AMPIPS enables us to specify the flight courses to be parallel with the wind direction measured *in situ* to avoid cross winds, as shown in Fig. 2 and 3.

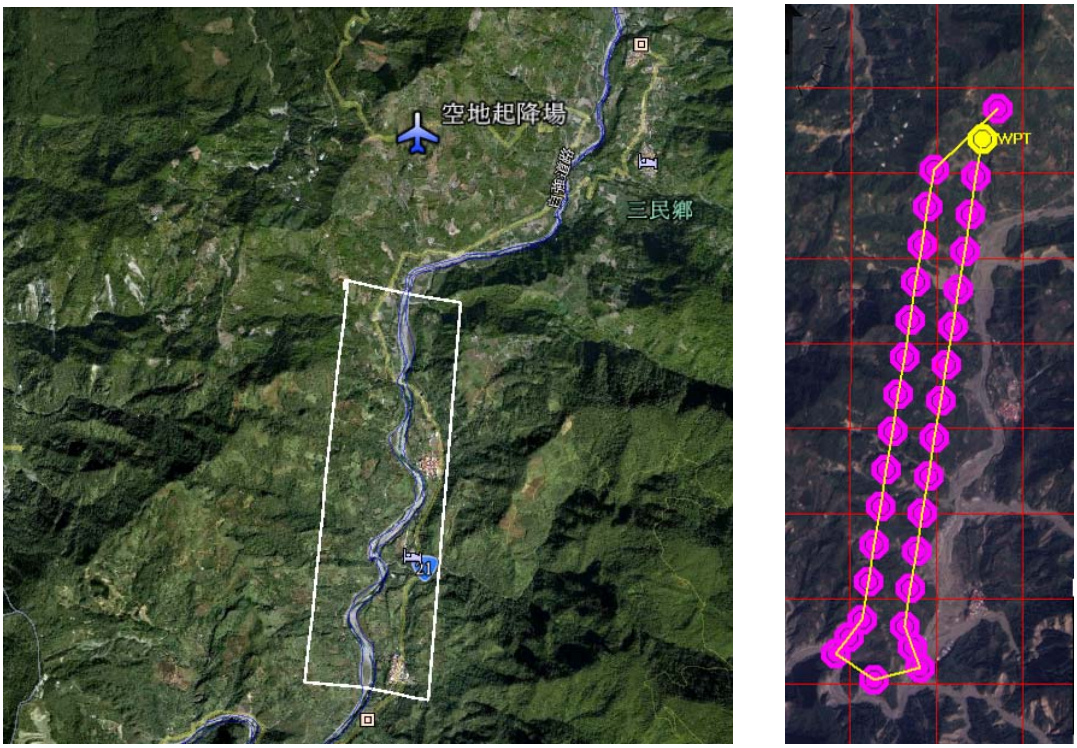


Figure 2. (A) Namasha area. (B) Flight plan made by AMPIPS.


Figure 3. (A) Laonung area. (B) Flight plan made by AMPIPS.

### 2.2 Camera calibration

AMPIPS allows the user to select the camera type and the calibration parameters of lens distortion. The self-calibration approach proposed by Fraser (1997) is employed to calculate the amount of distortion for each pixel, based on the following equation:

$$\Delta x = -x_0 - \frac{\bar{x}}{c}\Delta c + \bar{x}r^2K_1 + \bar{x}r^4K_2 + \bar{x}r^6K_3 + (2\bar{x}^2 + r^2)P_1 + 2P_2\bar{x}\bar{y} + b_1x + b_2y,$$

$$\Delta y = -y_0 - \frac{\hat{y}}{c}\Delta c + \bar{y}r^2K_1 + \bar{y}r^4K_2 + \bar{y}r^6K_3 + 2P_1\bar{x}\bar{y} + (2\bar{y}^2 + r^2)P_2,$$

where $\bar{x} = (x - x_p)$, $\bar{y} = (y - y_p)$, $r = \sqrt{\bar{x}^2 + \bar{y}^2}$, $c$ is the focal length. Table 2 lists the specification of Pentax W90 and Sony NEX-5 that are used as the payload. Table 3 gives their lens distortion parameters, including principal point deviation $x_p$ and $y_p$, decentric lens distortion $P_1$ and $P_2$, radial lens distortion $K_1$, $K_2$ and $K_3$.

TABLE 2. SPECIFICATION OF PENTAX W90 AND SONY NEX-5

| Camera<br>Specification | Pentax W90 | Sony NEX-5 |
|---|---|---|
| Effective pixels | 12,100,000 | 14,200,000 |
| Sensor Size | 6.16mm × 4.62mm | 23.4mm × 15.6mm |
| CCD unit size | 0.00154mm × 0.00154mm | 0.005096mm × 0.005105mm |
| Maximum resolution | 4000 × 3000 | 4592 × 3056 |
| Weight (without battery) | 144 g | 229 g |
| Weight (with battery) | 200 g | 410 g |

TABLE 3. DISTORTION PARAMETERS OF PENTAX W90 AND SONY NEX-5

| Camera<br>Parameters | Pentax W90 | Sony NEX-5 |
|---|---|---|
| focal length $c$ | 4.927665 mm | 15.833950 mm |
| Principal point deviation $x_p$ | -0.052341 mm | -0.102711 mm |
| Principal point deviation $y_p$ | 0.086146 mm | 0.040861 mm |
| Decentric Lens Distortion $P_1$ | 4.0015e-04 | 2.3056e-05 |
| Decentric Lens Distortion $P_2$ | -8.9581e-04 | -4.6168e-05 |
| Radial Lens Distortion $K_1$ | 3.5959e-04 | 2.8234e-04 |
| Radial Lens Distortion $K_2$ | -4.3294e-05 | -1.5239e-06 |
| Radial Lens Distortion $K_3$ | 2.0716e-06 | -2.3940e-11 |

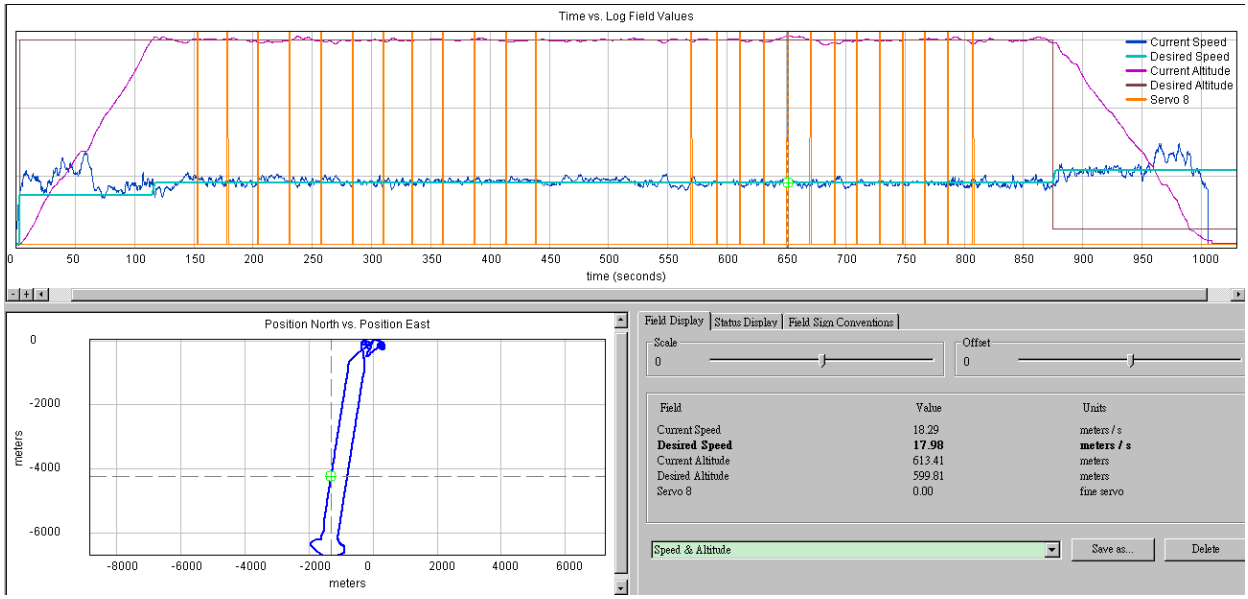


Figure 4. Flight log taken at Namasha area on 17 June 2011.

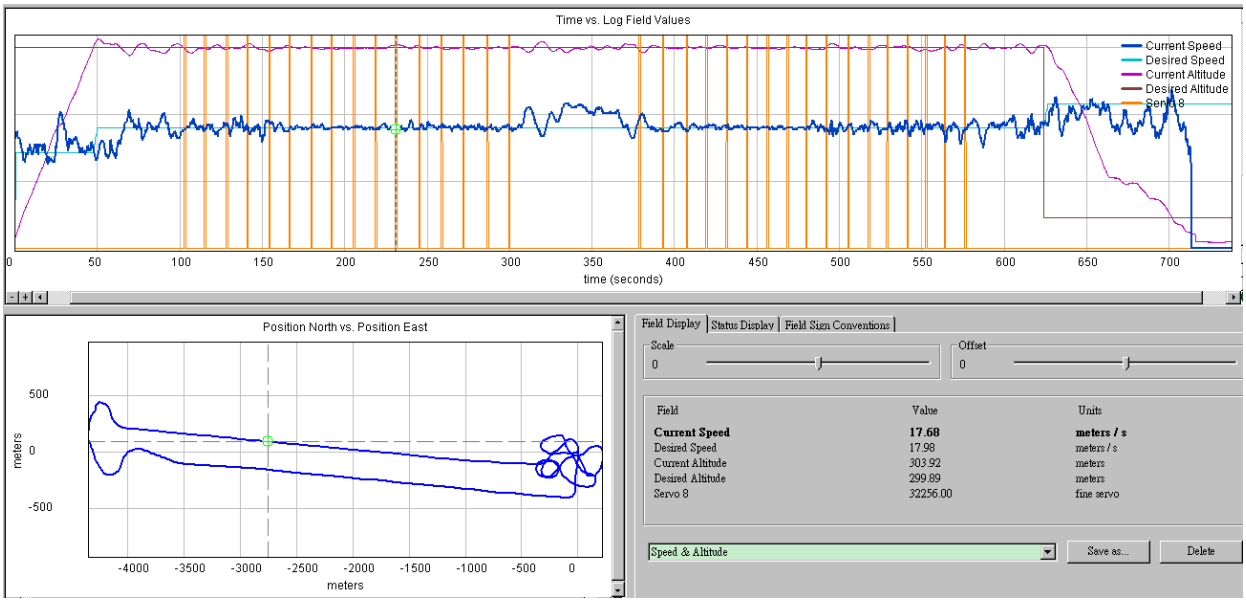

Figure 5. Flight log taken at Laonung area on 9 June 2011.

### 2.3 Flight log

Figure 4 and 5 shows the flight logs taken during two flights at Namasha and Laonung area, respectively. The flight routes are rather smooth. The servo 8 is controlled at approximately equal intervals to ensure the certain amount of overlaps can be achieved between all consecutive photos. A total of 22 and 32 photos were taken during two flights at Namasha and Laonung area, respectively.

## 3. IMAGE PROCESSING

### 3.1 Orthorectification

According to the flight plan, the base map/image can be cut into a set of reference images. Each reference image corresponds to one photo that would be taken by CropCam® during this flight mission. Comparing each projected-photo to its corresponding reference image, the user can select three pairs of conjugate points (CPs). An iterated calculation would be conducted to get the optimized solution of the GPS/INS data that minimize the difference between the projected coordinates and the readings from the reference image. The DTM of both study areas can be cut into a set of reference DTM too, each corresponds to one photo that is taken by CropCam® during this flight mission. With this reference DTM and three pairs of conjugate points, a detailed relief displacement of each pixel can be calculated. The calibrated-photo, therefore, can be orthorectified to the ortho-photo. Figure 6 gives one example of the original photo taken at Laonung area, the orthorectifed photo, and the orthorectified photo overlaid on DTM.

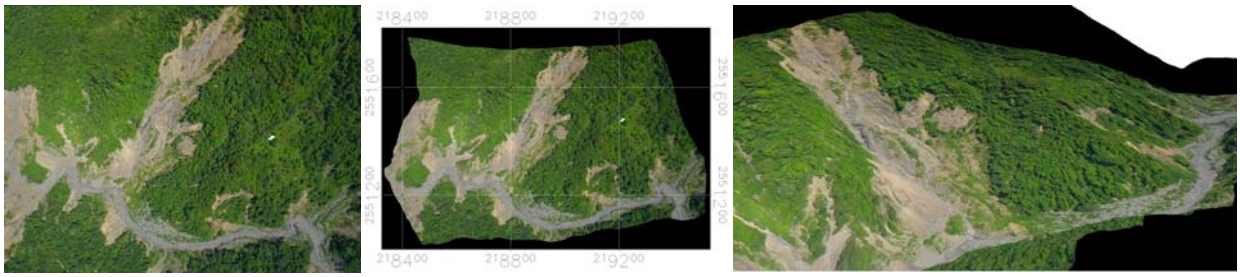
Figure 6. One example of (a) the original photo taken at Laonung area, (b) the orthorectifed photo, and (c) the orthorectified photo overlaid on DTM.

### 3.2 Mosaic

Since all ortho-photos have been orthorectified, they can be stitched to a seamless and color-balanced mosaic using the third-party photo-stitching software. By specifying the coordinates of three points referenced from the base map/image, the mosaic image can be geo-referenced to the ortho product, as shown in Figure 7 and 8.

Figure 7. The seamless and color-balanced mosaic of all photos taken at Namasha area.


Figure 8. The seamless and color-balanced mosaic of all photos taken at Laonung area.

### 3.3 Distribution through Web-GIS platform

One important factor in the effective response to slope hazards with UAV photos is the distribution of all UAV photos through Web-GIS platform. Among the various commercial platforms available for this purpose, we chose to use Google Earth, which has the largest number of users all over the world (Liu and Chen 2011). To support the requests from the general public and government officials, we employed the super-overlay technique to convert each UAV mosaicked image to a set of tiled images with different levels of details. Depending on the region browsed by the user, only those tiled images that fall within the region of interest need to be loaded and displayed on the web. With this type of processing, a large mosaicked image can be browsed by a number of Internet users simultaneously. Figure 9 gives the screen shot of both Formosat-2 image (2m) and UAV image (25cm) that we published on Multistage Remote Sensing Geospatial Information System (http://geodac.ncku.edu.tw/swcb/multistage.aspx).

## 4. PLANIMETRIC ACCURACY ASSESSMENT

Comparing with the 18 check points identified on the 25-cm resolution aerial orthophoto, the best accuracy of the highest level of geo-referenced product can achieve 6.3 pixels (1.58m) at Namasha area. Comparing with the 6 check points identified on the 25-cm resolution aerial orthophoto, the best accuracy of the highest level of geo-referenced product can achieve 14.72 pixels (3.68m) at Laonung area. A detailed description of the planimetric accuracy assessment can be referred to (NCKU Research And Development Foundation 2011).

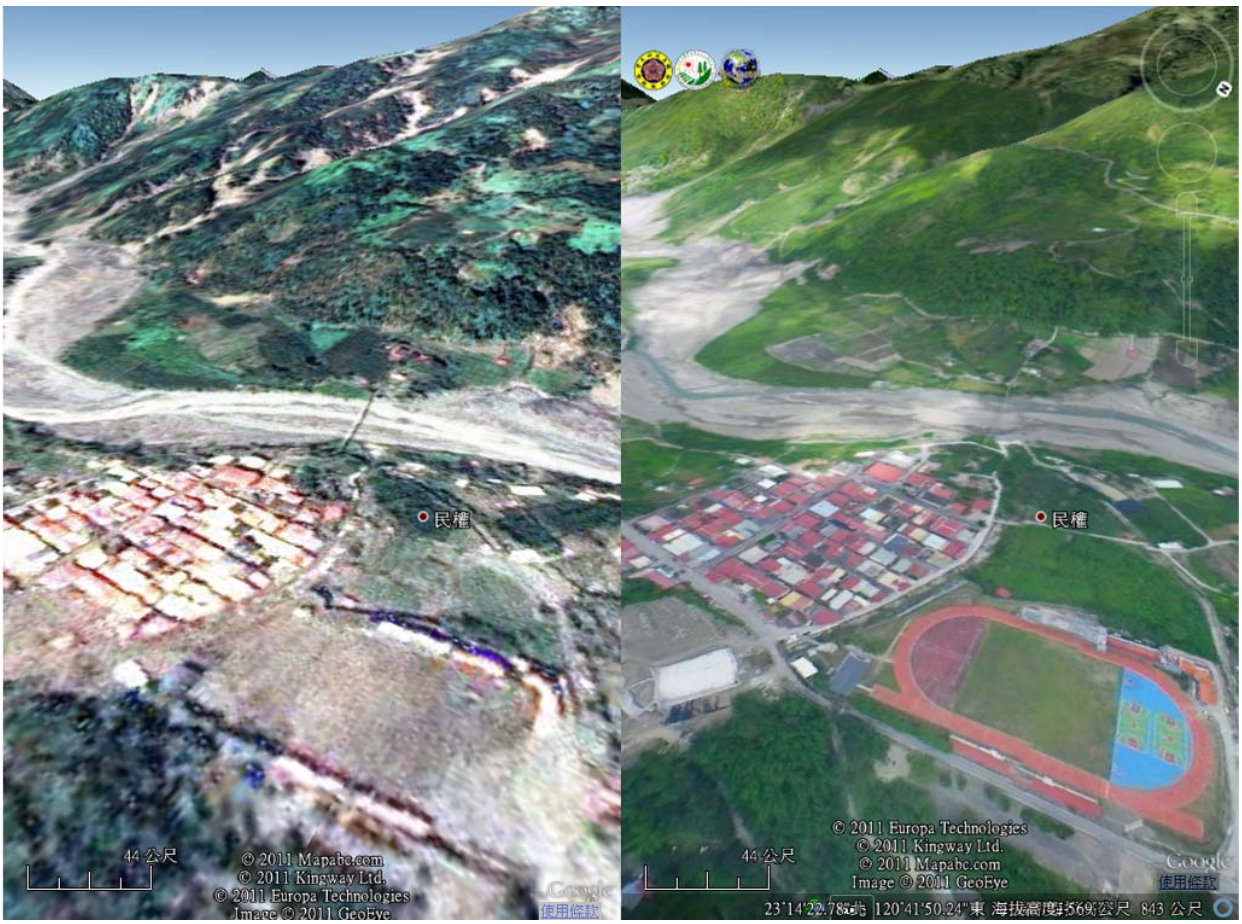

Figure 9. The screen shot of (a) Formosat-2 image (2m) and (b) UAV image (25cm) published on Multistage Remote Sensing Geospatial Information System (http://geodac.ncku.edu.tw/swcb/multistage.aspx).

## 5. CONCLUDING REMARKS

This research demonstrates that the orthorectified image of slope hazards can be rapidly generated using a low-cost UAV with AMPIPS, and the result can be shared and browsed in 3D fashion through the internet. AMPIPS serves as a fast and reliable approach to georeferencing photos/data acquired from low-cost UAV, such as CropCam®. This would play one of the key roles of blooming the civilian market of low-cost UAV. The AMPIPS is available through contact with National Cheng Kung University Technology Licensing and Business Incubation Center (TLBIC) (http://www.tlo.ncku.edu.tw/f_about_us_e.html)

ACKNOWLEDGEMENT

This research was supported by the National Science Council of the Republic of China, Taiwan, under Contract No. NSC-100-2611-M-006-002 and the Soil and Water Conservation Bureau under Contract No. 1000223050.

REFERENCES

Jones IV, George Pierce, Leonard G. Pearlstine, and H. Franklin Percival. 2006. An Assessment of Small Unmanned Aerial Vehicles for Wildlife Research. *Wildlife Society Bulletin* 34 (3):750-758.

Liu, Cheng-Chien. 2011. Multi-level georeferencing of photos acquired from a low-cost unmanned aerial vehicle.submitted.

Zhou, Gouqing, Chaokui Li, and Penggen Cheng. 2005. Unmanned Aerial Vehicle (UAV) Real-time Video Registration for Forest Fire Monitoring. *IEEE Transactions on Geoscience and Remote Sensing*.

Fraser, Clive S. 1997. Digital camera self-calibration. *ISPRS Journal of Photogrammetry & Remote Sensing* 52:149-159.

Liu, Cheng-Chien, and Nai-Yu Chen. 2011. Responding to natural disasters with satellite imagery. *SPIE Newsroom*.

NCKU Research And Development Foundation. 2011. Multi-scale remote sensing information system data establishment, expansion and maintenance. Midterm report.